3D Visualisation of trans-syncytial nanopores provides a pathway for paracellular diffusion across the human placental syncytiotrophoblast

Short title: Trans-syncytial nanopores

Rohan M Lewis*[1,3], Harikesan Baskaran[4], Jools Green[1], Stanimir Tashev[2], Eleni Paleologou[1], Emma M Lofthouse[1], Jane K Cleal[1,3], Anton Page[2], David S Chatelet[2], Patricia Goggin[2], Bram G Sengers[3,4]

[1] University of Southampton, Faculty of Medicine

[2] University of Southampton, Faculty of Medicine, Biomedical Imaging Unit

[3] University of Southampton, Institute for Life Sciences

[4] University of Southampton, Faculty of Engineering and Physical Sciences

Data availability statement: Underlying SBFSEM data is available on the Electron Microscopy Public Image Archive https://dx.doi.org/10.6019/EMPIAR-10967

***Corresponding Author**: Rohan M Lewis, MP 887, IDS Building University of Southampton, Faculty of Medicine, Southampton General Hospital, rohan.lewis@soton.ac.uk

Abstract

The placental syncytiotrophoblast, a syncytium without cell-cell junctions, is the primary barrier between the mother and the fetus. Despite no apparent anatomical pathway for paracellular diffusion of solutes across the syncytiotrophoblast size-dependent paracellular diffusion is observed. Here we report data demonstrating that the syncytiotrophoblast is punctuated by trans-syncytial nanopores (TSNs). These membrane-bound TSNs directly connect the maternal and fetal facing sides of the syncytiotrophoblast, providing a pathway for paracellular diffusion between the mother and fetus. Mathematical modelling of TSN permeability based on their 3D geometry suggests that 10-60 million TSNs per cm^3 of placental tissue could explain experimentally observed placental paracellular diffusion. TSNs may mediate physiological hydrostatic and osmotic pressure homeostasis between the maternal and fetal circulations but also expose the fetus to pharmaceuticals, environmental pollutants and nanoparticles.

Introduction

Potentially harmful molecules and particulates can cross the placenta and impair fetal development. However, the mechanism by which this occurs is unclear [1, 2]. Understanding the mechanism of trans-placental diffusion is necessary to identify risks and prevent long-term consequences of exposures, which may adversely affect fetal and postnatal health [3].

The primary placental barrier is the syncytiotrophoblast, a continuous syncytial monolayer covering the villi at the maternal-fetal interface. Despite the absence of an anatomical pathway for trans-placental diffusion, there is physiological evidence for size-dependent paracellular solute diffusion [4, 5]. Trans-syncytial channels, or nanopores, have been proposed as diffusion mediators, however continuous full-width nanopores have not been demonstrated in human placenta [6].

This serial block-face scanning electron microscopy (SBFSEM) study reconstructs 3D placental ultrastructure and demonstrates the presence of trans-syncytial nanopores (TSNs) in human placenta.

Methods

Term placental tissue was collected after delivery from uncomplicated pregnancies with written informed consent and ethical approval from the Southampton and Southwest Hampshire Local Ethics Committee (11/SC/0529).

Villous samples from 8 placentas were processed and imaged using TEM or SBFSEM as described previously [7]. In SBFSEM stacks continuous TSNs with a clear connection between the apical and basal membranes were identified (Supplementary figure S1). Near-continuous TSNs were also identified which had connections to both the apical microvillous and basal plasma membranes but contained discontinuities along the length of the nanopore. Unilateral nanopores, ultrastructurally similar to TSNs but opened from either the apical or basal plasma membrane without connecting to the opposite membrane were identified. Regions containing TSNs were manually segmented in Avizo v2019.4 (ThermoFisher, Eindhoven).

Modelling of nanopore diffusive transfer capacity

The magnitude of the diffusive flux J_{pore} [mol/s] through a pore of uniform cross section is given by:

$$J_{pore} = DA_{pore}\frac{|\Delta C|}{L_{pore}} \qquad \text{Eq. 1}$$

where D [m^2/s] is the diffusion coefficient, A_{pore} [m^2] the pore cross sectional area, ΔC [mol/m^3] the concentration difference over the pore and L_{pore} [m] the pore length. In terms of the permeability surface area product PS_{pore} [m^3/s]:

$$J_{pore} = PS_{pore}\Delta C \quad \text{, where } PS_{pore} = \frac{DA_{pore}}{L_{pore}} \qquad \text{Eq. 2}$$

Since the pore cross sectional area varies, 3D image-based simulations were used to calculate the effective area-over-length ratio A_{pore}/L_{pore} [m] as a measure for the effect of pore geometry on diffusive transfer, independent of the solute studied.

Segmented image stacks were imported in Simpleware ScanIP (P-2019.09; Synopsys, Inc., Mountain View, USA). Voxels were resampled isotropically so that the x and y pixel size matched the z axis spacing. Pores were meshed using linear tetrahedral elements, with the final number of elements ranging from 1.4–38×10^5.

Steady state diffusion simulations were performed in COMSOL Multiphysics (v5.5; COMSOL AB, Stockholm, Sweden). Since A_{pore}/L_{pore} does not depend on the choice of parameters, $D = 1$ m^2/s was used and a fixed concentration gradient $\Delta C = 1$ mol/m^3 was imposed by constant concentration boundary conditions on the inlet and outlet surface of the pore , while the remaining external surface was subject to no-flux conditions.

After simulations, the magnitude of the diffusive flux J_{pore} given by the integral of the normal solute flux over the pore inlet or outlet cross sectional area, was then used to calculate the effective pore area-over-length ratio A_{pore}/L_{pore} based on Eq. 1.

Results

Trans-syncytial nanopores

This study manually inspected 14 SBFSEM image stacks from five different placentas to identify trans-syncytial nanopores (TSNs) defined as membrane lined pores connecting the apical and basal plasma membranes of the syncytiotrophoblast. These stacks consisted of 7487 SBFSEM images, representing a total volume of 0.000002 cm^3.

Ten continuous TSNs were identified from three different placentas (figure 2). In addition, 20 near-continuous TSNs were identified, with examples in all five placentas studied. In two cases, these near-continuous TSNs were highly complicated with branches, multiple dilations, and blind ends (figure 3b). Finally, 25 unilateral nanopores were identified arising from either the apical (n = 17) or basal (n = 8) plasma membrane of the syncytiotrophoblast but not connecting to the opposing plasma membrane.

The TSNs were structurally heterogeneous, ranging from simple thin tubes connecting the apical and basal syncytiotrophoblast plasma membranes to complex branching structures with multiple dilated regions and blind ends (figures 3b, 3e and 4).

The lumens of TSNs typically had low electron density, consistent with a primarily fluid filled pore (figure 2). However, some TSNs and regions of TSNs were observed with higher electron density indicating diffuse contents (figure 2e).

On the basal membrane, continuous and near-continuous TSN were observed opening adjacent to basal lamina in 16 cases and regions adjacent to cytotrophoblast in 14 cases.

Of the ten continuous TSNs, eight contained membrane-bound inclusions which, surrounded by the nanopore, formed double-membrane structures (figure 3). Inclusions were also observed in the majority of near-continuous and unilateral nanopores. In three cases, the inclusions appeared to be trophoblastic in origin. In the first case, the inclusion on the apical side appeared to be connected to the syncytiotrophoblast by at least one thin stalk of cytoplasmic material (figure 3a). At the available resolution, it was not clear whether other inclusions were also engulfed syncytiotrophoblast. In two cases, an inclusion on the basal side of the placenta was a clear-cut protrusion from an underlying cytotrophoblast cell (figure 3d). Another less commonly observed feature associated with TSNs were thin nanopores within the syncytiotrophoblast, where two closely adjacent membranes were joined by desmosome like adhesions (Supplementary figure S2). A movie showing a TSN reconstructed in 3D (Supplementary data S3) and another showing nanopore lumen highlighted in sequential sections (Supplementary data S4) are available in supplemental data.

Modelling diffusion through TSNs

Depending on their geometry, individual nanopores display a large variation in estimated effective A_{pore}/L_{pore} from 0.14 x 10^{-8} m to 2.08 x 10^{-8} m (figure 4j). The effective A_{pore}/L_{pore} ratio based on the results of the computational simulations of the ten pores, as depicted in figure 3, was in the order of 10 nm (8.5 ± 7.2 × 10^{-9} m, mean ± SD). By

multiplying the mean effective A_{pore}/L_{pore} ratio with the diffusion coefficient for particular solutes using Eq. 2, the average permeability surface area products for a single pore could then be calculated (table 1). Dividing the corresponding experimentally observed placental permeability surface area products by the value for a single pore, resulted in placental pore number estimates between 13 and 59 million pores per gram.

Discussion

The demonstration of nanoscale pores punctuating the syncytiotrophoblast challenges our understanding of the placenta as a barrier. It suggests that rather than being a continuous physical barrier between mother and fetus, the syncytiotrophoblast is a molecular sieve facilitating diffusion of small solutes via active maintenance of TSNs. These solutes may include nutrients and toxins, so this transfer route may have profound implications for the fetus.

TSNs were structurally heterogeneous, including simple tubes, tubes with dilated regions and branched structures with blind ends. Many TSNs also contained inclusions of membrane-bound material, in three cases trophoblastic in origin but in most cases the origin was unclear. Some TSNs had multiple openings to the syncytiotrophoblast apical microvillous or basal membranes. The near-continuous and unilateral nanopores are likely in the process of formation, degradation or remodelling. It is also possible that near-continuous TSNs are continuous but that the connections were too thin to observe.

There was a wide range in calculated permeability parameters for the modelled TSNs, with diffusion through the most permeable being 10 x greater than the least permeable. As might be expected, shorter, wider TSNs had the greatest permeability while the longer TSNs had the lowest permeability (excluding the TSN with multiple apical and basal openings).

Molecules such as IgG or nanoparticles such as ultrafine diesel exhaust could infiltrate? most regions of the TSNs, but the diameter would sterically hinder their transfer. TSN diameter might be a significant barrier to the transfer of large molecules unless an additional biological mechanism facilitates this transfer.

Further research is required to determine TSN densities in placental tissue. An initial approximation for the TSN density was obtained by dividing the number of observed TSNs (10 continuous or 30 including continuous and near-continuous TSNs) by the imaged volume of 0.00000017 cm^3. This initial approximation for TSN density is 58 million TSNs per cm^3, and including near-continuous TSNs is 162 million/cm^3. This estimate is in line with modelled estimate of the number of TSNs required to mediate transfer of known paracellular markers such as inulin and creatinine.

The physiological role of TSNs is likely to include the maintenance of ionic and osmotic homeostasis between mother and fetus. Diffusion of ions and bulk fluid flow would balance osmotic and pressure gradients that could build up across an impermeable placenta. TSNs may also facilitate the placental transfer of nutrients, such as glucose, with

maternal to fetal gradients to the fetus [8]. However, the physiological roles of TSNs may come at the cost of allowing non-selective transfer of potentially harmful substances.

In conclusion, this study has demonstrated the existence of TSNs providing a non-selective diffusion pathway across the placenta. These TSNs may allow pharmacological drugs, environmental toxins and even particulate pollutants across the syncytiotrophoblast. Accurately determining the density of TSNs in healthy pregnancy is necessary to confirm the capacity of TSNs to mediate transfer. Furthermore, establishing the density of TSNs in disease may provide novel insights into disease processes.

Acknowledgements: This work was supported by BBSRC project grant BB/R002762/1. Equipment in the Biomedical Imaging Unit was supported by MR/L012626/1 Southampton Imaging under MRC UKRMP Funding.

Competing interests: None

Author contributions CREDIT statement

Rohan M Lewis: Conceptualization, Funding Acquisition, Investigation, Supervision, Writing – Original Draft Preparation, Writing – Review & Editing.

Harikesan Baskaran: Investigation, Formal Analysis, Writing – Review & Editing.

Jools Green: Investigation, Writing – Review & Editing.

Stanimere Tashev: Investigation, Writing – Review & Editing.

Eleni Paleologou: Investigation, Writing – Review & Editing.

Emma M Lofthouse: Resources, Writing – Review & Editing.

Jane K Cleal: Funding Acquisition, Supervision, Writing – Review & Editing.

Anton Page: Funding Acquisition, Methodology, Supervision, Writing – Review & Editing.

David S Chatelet: Formal Analysis, Supervision, Writing – Review & Editing.

Patricia Goggin: Methodology, Supervision, Writing – Review & Editing.

Bram G Sengers: Funding Acquisition, Formal Analysis, Supervision, Writing – Original Draft Preparation, Writing – Review & Editing.

197 **References**

198 1. Lofthouse EM, Torrens C, Manousopoulou A, Nahar M, Cleal JK, O'Kelly IM, et al.
199 Ursodeoxycholic acid inhibits uptake and vasoconstrictor effects of taurocholate in human
200 placenta. FASEB journal : official publication of the Federation of American Societies for
201 Experimental Biology. 2019;33(7):8211-20. Epub 2019/03/30. doi: 10.1096/fj.201900015RR.
202 PubMed PMID: 30922127; PubMed Central PMCID: PMCPMC6593889.
203 2. Bove H, Bongaerts E, Slenders E, Bijnens EM, Saenen ND, Gyselaers W, et al. Ambient
204 black carbon particles reach the fetal side of human placenta. Nat Commun.
205 2019;10(1):3866. Epub 2019/09/19. doi: 10.1038/s41467-019-11654-3. PubMed PMID:
206 31530803; PubMed Central PMCID: PMCPMC6748955.
207 3. Lewis RM, Demmelmair H, Gaillard R, Godfrey KM, Hauguel-de Mouzon S, Huppertz
208 B, et al. The Placental Exposome: Placental Determinants of Fetal Adiposity and Postnatal
209 Body Composition. Annals of Nutrition and Metabolism. 2013;63(3):208-15. doi:
210 10.1159/000355222. PubMed PMID: WOS:000329057400005.
211 4. Thornburg KL, Burry KJ, Adams AK, Kirk EP, Faber JJ. Permeability of placenta to
212 inulin. American journal of obstetrics and gynecology. 1988;158(5):1165-9. Epub
213 1988/05/01. doi: 10.1016/0002-9378(88)90246-3. PubMed PMID: 3369499.
214 5. Bain MD, Copas DK, Taylor A, Landon MJ, Stacey TE. Permeability of the human
215 placenta in vivo to four non-metabolized hydrophilic molecules. The Journal of physiology.
216 1990;431:505-13. PubMed PMID: 2129229; PubMed Central PMCID: PMCPMC1181787.
217 6. Kertschanska S, Kosanke G, Kaufmann P. Pressure dependence of so-called
218 transtrophoblastic channels during fetal perfusion of human placental villi. Microscopy
219 research and technique. 1997;38(1-2):52-62. doi: 10.1002/(SICI)1097-
220 0029(19970701/15)38:1/2<52::AID-JEMT7>3.0.CO;2-W. PubMed PMID: 9260837.
221 7. Palaiologou E, Etter O, Goggin P, Chatelet DS, Johnston DA, Lofthouse EM, et al.
222 Human placental villi contain stromal macrovesicles associated with networks of stellate
223 cells. Journal of anatomy. 2020;236(1):132-41. Epub 2019/09/13. doi: 10.1111/joa.13082.
224 PubMed PMID: 31512233.
225 8. Day PE, Cleal JK, Lofthouse EM, Hanson MA, Lewis RM. What factors determine
226 placental glucose transfer kinetics? Placenta. 2013;34(10):953-8. doi:
227 10.1016/j.placenta.2013.07.001. PubMed PMID: WOS:000330331500016.
228 9. Atkinson DE, Robinson NR, Sibley CP. Development of passive permeability
229 characteristics of rat placenta during the last third of gestation. The American journal of
230 physiology. 1991;261(6 Pt 2):R1461-4. Epub 1991/12/01. doi:
231 10.1152/ajpregu.1991.261.6.R1461. PubMed PMID: 1750569.
232 10. Collins MC, Ramirez WF. Transport through polymeric membranes. J Phys Chem
233 1979;83:2294–301. doi: https://doi.org/10.1021/j100480a022.

234

235 **Figures and tables**

236

237 ***Table 1: Estimated number of pores per gram required to explain the experimentally***
238 ***observed placental permeability surface area products.***

	D ($m^2\ s^{-1}$)	PS_{pore} ($m^3\ s^{-1}$)	$PS_{placenta}$ ($m^3\ s^{-1}\ g^{-1}$)	number of pores (g^{-1})
Inulin*	2.6×10^{-10}	2.20×10^{-18}	0.28×10^{-10}	13×10^{6}
CrEDTA*	7.0×10^{-10}	5.92×10^{-18}	1.06×10^{-10}	18×10^{6}
Mannitol*	9.9×10^{-10}	8.37×10^{-18}	2.50×10^{-10}	30×10^{6}
Creatinine**	12.9×10^{-10}	10.9×10^{-18}	6.41×10^{-10}	59×10^{6}

239 *Placental permeability surface area product data taken from Bain *et al.* (1990) [5] and diffusion coefficients
240 from Atkinson *et al.* (1991) [9]. ** Permeability surface area product calculated based on Cleal *et al.* (2007)
241 and diffusion coefficient from Collins *et al.* (1979) [10].

242

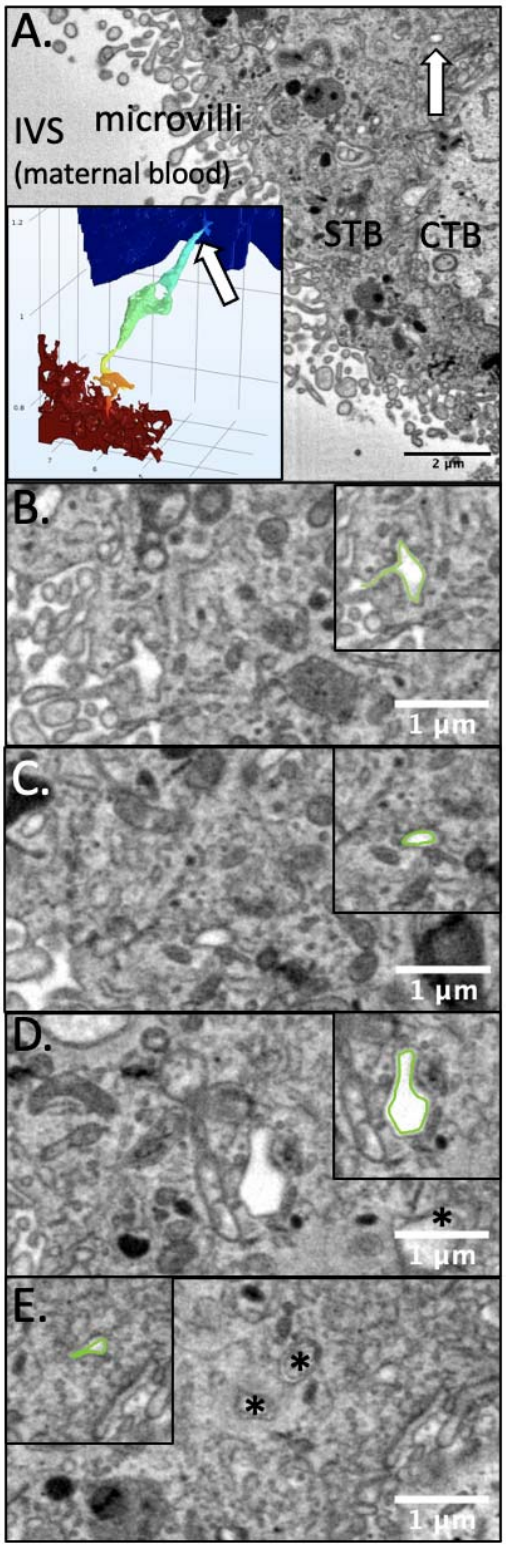

Figure 2, SBF SEM serial sectioning allows identification of TSNs crossing the human placental syncytiotrophoblast. A) An SBF SEM image showing a cross section of the syncytiotrophoblast (STB) from the maternal intervillous space (IVS) to the underlying cytotrophoblast (CTB). Within this image a cross section of a nanopore can be seen (white arrow) illustrating how difficult it would be to identify these structures from individual 2D images. The inset shows the nanopore reconstructed in 3D from 44 consecutive sections with the white arrow indicating where the section comes from and modelled solute concentration indicated by colour from high (red) to low (blue). **B)** the apical opening of the TSN with the inset showing this highlighted in green. **C)** A thin region of nanopore with the inset showing this highlighted in green. **D)** a dilated region of the nanopore with the inset showing this highlighted in green. In B, C and D the nanopore has a low electron density consistent with a fluid filled pore **E)** A region of nanopore where the lumen has a higher electron density than in other regions. The inset showing this cross section of the nanopore highlighted in green. This region is close to the end of the nanopore and the cytotrophoblast boundary can be seen bottom left. * Indicate inclusion bodies. A movie showing the nanopore reconstructed in 3D and another movie with the nanopore lumen highlighted in sequential sections can be seen in the supplemental material).

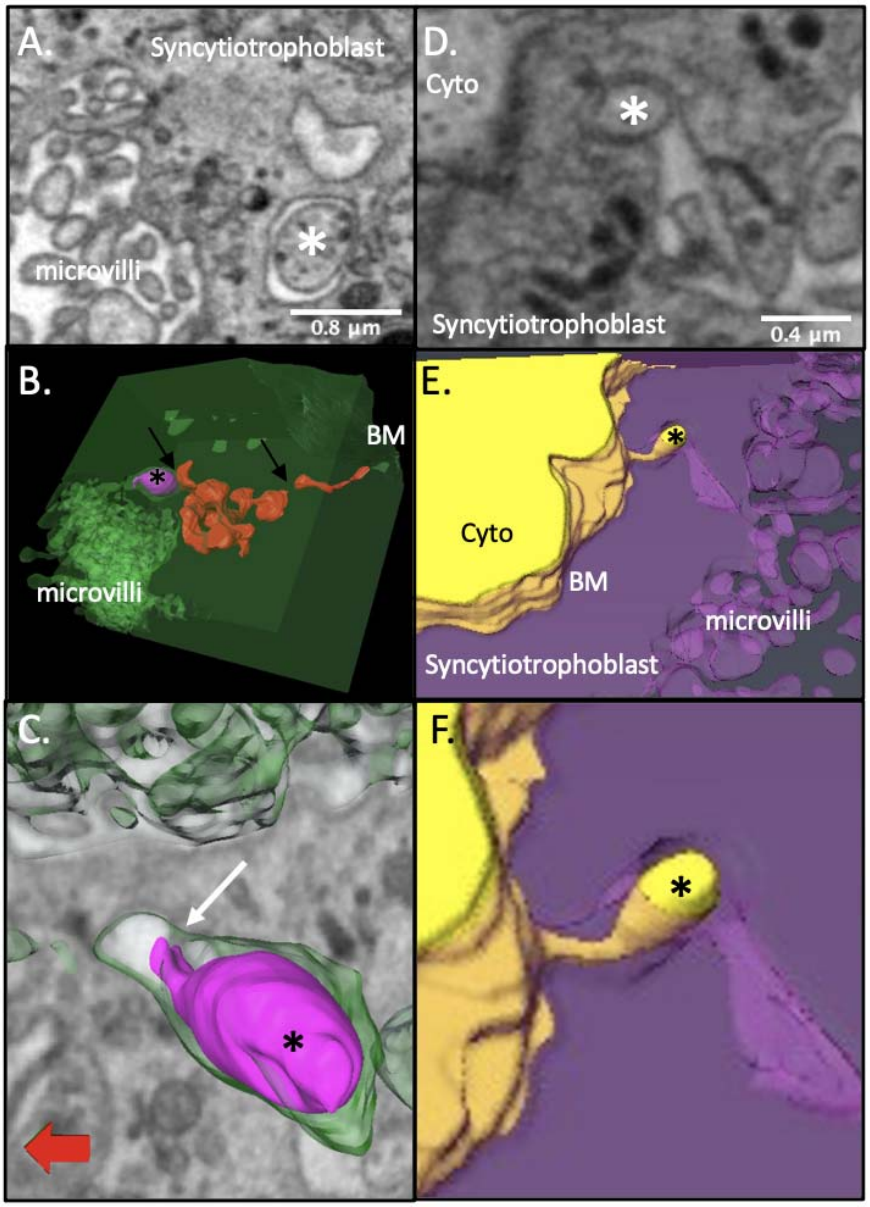

Figure 3, **Examples of TSN inclusions formed from engulfed syncytiotrophoblast or cytotrophoblast. A-C**) an apical nanopore inclusion body (*) was observed which appeared to be derived from the trophoblast (green). **A)** shows a SBF SEM image containing a cross section of a TSN inclusion. **B)** shows the same inclusion (pink) in 3D within a complex near-continuous TSN (red). This TSN has several discontinuities indicated by black arrows but gives the appearance of being part of a trans-syncytial network even if it does not form a complete pore. **C)** shows a higher power image of the inclusion which is continuous with the syncytiotrophoblast (green) via a small stalk (white arrow). **D-F)** An example of a TSN inclusion which is derived from the underlying cytotrophoblast (yellow). **D)** shows a SBFSEM image of the cytotrophoblast derived inclusion. **E)** shows the nanopore inclusion within a TSN with a relatively simple tubular structure. **F)** shows a higher power image of the cytotrophoblast derived inclusion.

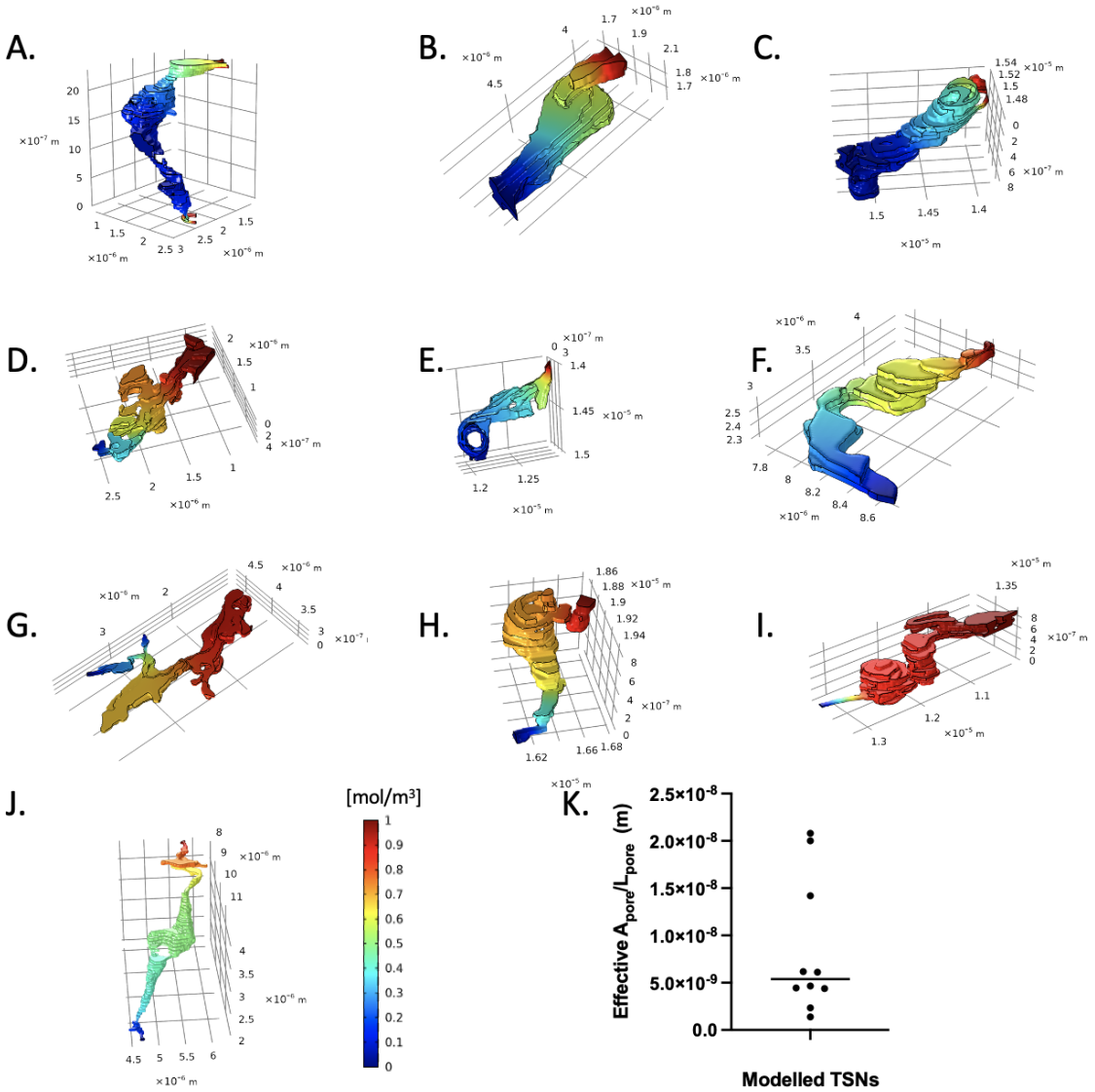

Figure 4, **Modelled solute concentration gradients within the continuous TSNs.** High concentrations (red) were applied to the maternal facing TSN opening, and concentration gradients are shown for diffusion through the channel. The molecular flux associated with these gradients was used to calculate the effective cross sectional surface area used to calculate permeability. **A-J)** show the nanopores presented in order of calculated permeability from highest to lowest. The apical opening is presented on top right and basal openings on the bottom or left. The TSN shown in A is a double pore with four apical and basal openings and a connection on the basal side which accounts for its higher permeability despite its longer length. Blind ends are present in D, I and G. TSN A has two openings to the microvillous membrane and two openings to the basal membrane of the syncytiotrophoblast. **J)** shows a scatterplot showing the distribution of permeabilities with the line indicating the median value.

Supplemental figures

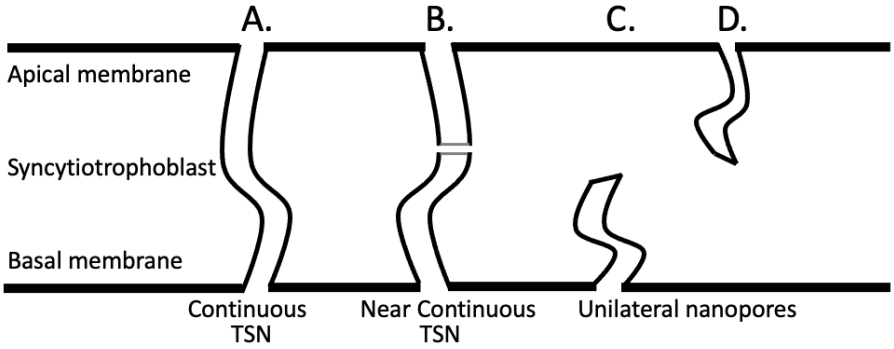

Figure S1, Classification of nanopores found in human placental syncytiotrophoblast. A, continuous TSNs connecting the apical and basal membrane without any breaks. **B,** near-continuous TSNs with sections connected to the apical and basal plasma membranes but contained discontinuities where no clear connection could be observed but the ends of the discontinuous sections were adjacent. **C & D.** Unilateral nanopores were ultrastructurally similar to TSNs but opened from either the apical or basal plasma membrane but without any apparent connection to the opposing membrane.

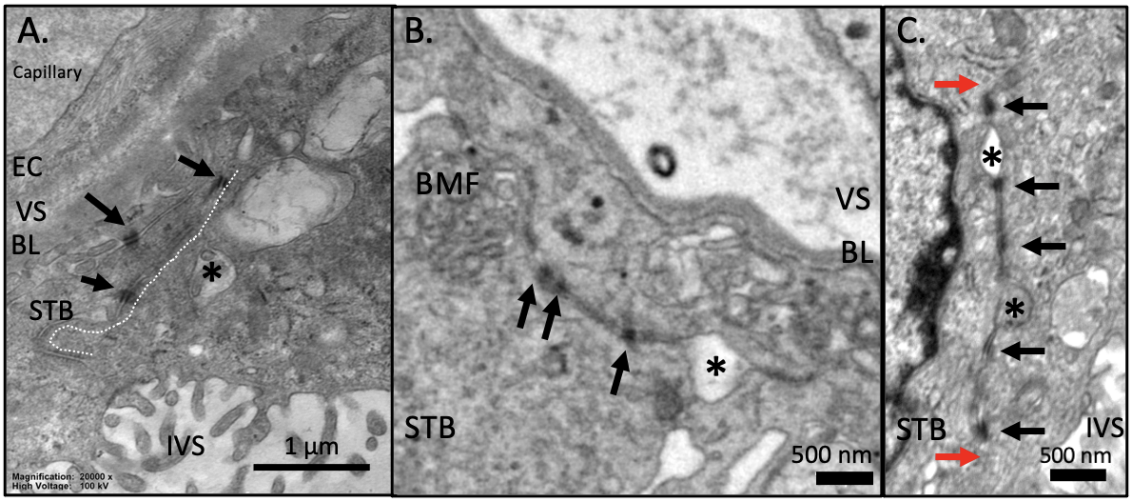

Figure S2, Desmosome associated nanopores. A) a TEM image of a desmosome associated nanopore traversing most of the width of the syncytiotrophoblast (white dotted line) and associated with dilation typical of TSNs (indicated by an *). **B)** an SBF SEM image of a desmosome associated nanopore connecting basal membrane folds to a TSN like opening (*). **C)** A TEM image of a desmosome associated nanopore which begins and ends in the same field of view (red arrows). This demonstrates that it is not a cell-cell junction as if this were the case it would need to intersect 2 sides of the image or be a circle. This channel contains an empty TSN like dilation (top*) and one which contains inclusion material (bottom*). EC = endothelial cell, VS = villous stroma, BL = basal lamina, STB = syncytiotrophoblast, BMF = basal membrane folds. IVS = intervillous space.